How to cite: *Angew. Chem. Int. Ed.* **2026**, *65*, e20032
doi.org/10.1002/anie.202520032

Polymer-Protein Conjugation ***Very Important Paper***

Tuning Polyacrylate Composition to Recognize and Modulate Fluorescent Proteins

Darwin C. Gomez, Swarnadeep Seth, Ronnie Mondal, Stephen J. Koehler, Jared G. Baker, Charles Plate, Ian C. Anderson, Mikayla R. Smith, Joey Gloriod, Morgan Gunter, Valerie V. Welborn, Sanket A. Deshmukh,* and C. Adrian Figg**

Abstract: Molecular definition is usually regarded as a prerequisite to achieve protein recognition and functional modulation, particularly for macromolecular interactions. Herein, we report that polymers with specific combinations of monomers arranged into random sequences [random hetero oligomers (RHOs)] can selectively bind to a model protein. Using green fluorescent protein (GFP) as a target, polyacrylates were developed that bound with nanomolar affinity and enhanced fluorescence by >100%. Purification of the polymerization product revealed subpopulations of compositions with distinct affinities and selectivity for GFP over a competing protein. Experimental and computational binding analyses confirmed that there are distinct RHO–GFP interactions, which are influenced by RHO chemical composition. These findings show that sequence-defined structures are not a prerequisite for selective protein recognition. Synthetic polymers can instead serve as scalable, tunable platforms for molecular recognition—representing a significant leap towards next-generation sensing, therapeutic, responsive, and catalytic materials in domains previously dominated by biologics or complex peptide scaffolds.

Introduction

Protein surfaces are chemically diverse and often show promiscuous interactions,[1,2] yet molecular recognition is usually restricted to well-defined structures (e.g., peptides, small molecules, proteins, oligonucleotides, oligosaccharides).[3–9] Synthetic polymers, widely used in commodity materials such as coatings and plastics,[10–14] remain significantly underexplored for protein recognition and modulation due to the prevailing emphasis for sequence definition and molecular purity as a prerequisite for binding.[15–17] Here, we show that readily accessible polymerization methods can be used to develop protein modulators, where sequence definition is not a necessity.

Polymers would provide a vast and tunable potential chemical design space for protein recognition and modulation, leading to new sensing, therapeutic, responsive, and/or catalytic materials. These materials would be scalable and modular alternatives compared to current methods of protein recognition (e.g., antibodies, aptamers, peptides, small molecules).[18–21] Random poly(meth)acrylate copolymers can stabilize proteins,[22,23] mimic cytoplasm compositions,[24,25] or garner catalytic and/or folded structures,[26–28] suggesting that sequence definition is not a prerequisite for functional protein interactions.[29–31] Despite these advances, polymers have not been shown to achieve protein binding and modulation that is comparable to aptamers, peptides/peptidomimetics, phage display, or de novo protein design.[4,5,32,33]

Strategies for targeting protein surfaces recapitulate amino-acid binding interactions (e.g., hot spot, hydrophobic, or ionic interactions) into proteins,[34,35] peptides,[32,36] peptidomimetics,[37–39] molecular analogs,[4] aptamers,[8,40] or biomolecule-templated nanomaterials.[26,41–44] However, synthetic polymers remain significantly underexplored for protein recognition and modulation due to the prevailing emphasis for sequence definition and molecular purity as a prerequisite for binding.[15–17,45] Schraeder, Thayumanavan,

[*] D. C. Gomez, R. Mondal, S. J. Koehler, J. G. Baker, I. C. Anderson, M. R. Smith, J. Gloriod, M. Gunter, V. V. Welborn, C. A. Figg
Macromolecules Innovation Institute and Department of Chemistry, Virginia Tech, Blacksburg, Virginia 24061, USA
E-mail: vwelborn@vt.edu
figg@vt.edu

D. C. Gomez, S. J. Koehler, J. G. Baker, I. C. Anderson, M. R. Smith, J. Gloriod, M. Gunter, C. A. Figg
Virginia Tech Center for Drug Discovery, Virginia Tech, Blacksburg, Virginia 24061, USA

D. C. Gomez
Department of Chemistry, Eastern Visayas State University, Tacloban City 6500, Philippines

S. Seth, C. Plate, S. A. Deshmukh
Department of Chemical Engineering, Virginia Tech, Blacksburg, Virginia 24061, USA
E-mail: sanketad@vt.edu

Additional supporting information can be found online in the Supporting Information section

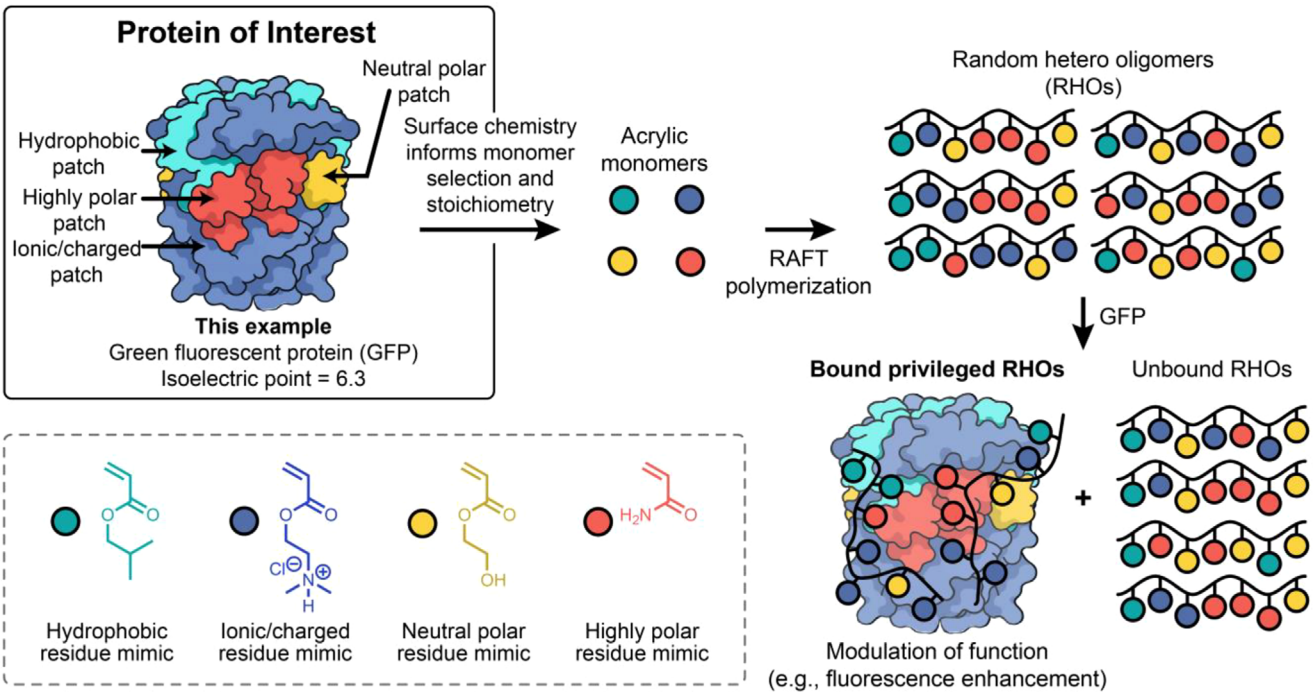

Figure 1. Design of random hetero oligomers (RHOs) based on green fluorescent protein (GFP) surface chemistry. The chemical properties of protein patches can be used to identify acrylic monomers, which are polymerized via reversible-deactivation radical polymerization techniques [e.g., reversible addition-fragmentation chain transfer (RAFT) polymerization].

and Rotello pioneered using reversible-reactivation radical polymerization (RDRP) to prepare protein-binding polymers using protein-specific monomers (e.g., bis-phosphonate monomers).[46–49] Recently, random hetero polymers [RHPs, typical degree of polymerization (DP) >50] developed by Xu and others show that random copolymers can stabilize proteins,[50,51] mimic protein functions,[25,52] or serve as excipients for drug delivery.[53] Despite these advances, polymers with highly-tunable protein interactions and resultant functional modulation (e.g., gain-of-function)[29,54–57] are absent.

As a proof-of-concept, we used the RDRP technique reversible addition-fragmentation chain transfer (RAFT) polymerization[58–60] to synthesize polyacrylates where a subset of privileged compositions were expected to show preferential binding to the surface of the model protein green fluorescent protein (GFP) through specific chemical interactions (Figure 1). This approach enables the rapid generation of a library of polyacrylate sequences, compositions, and molecular weights in a single polymerization. These polymers can be further enriched through straightforward purification to identify strong-binding candidates. These random hetero oligomers (RHOs) incorporate chemical interactions commonly used in protein-binding designs and are on the same length scale as the target protein surface, further facilitating a binding interaction. This binding acts like an allosteric regulator,[61] enhancing protein function via surface-specific interactions. While point mutations can be used to increase GFP fluorescence,[62,63] our approach modulates protein function without altering the sequence. Importantly, RHOs are not intended to be sequence-defined structures. Rather, the inherent polyacrylate structural and compositional diversity resulting from RDRP is leveraged to enhance RHO–protein binding.

Results and Discussion

Chemical Dependence Of RHOs Modulating Protein Function

We initially modeled RHO compositions after the split peptide composition of a truncated GFP structure (Figures S1,S2) due to the promiscuity of these interactions.[64,65] Attempts to achieve gain-of-function restoration of the truncated GFP fluorescence were largely unsuccessful (Figures S3–S5). However, control experiments with the intact GFP and RHOs showed gain-of-function fluorescence increases (Figure S6). Based on these results, we expected that monomers mimicking amino acids would bind to the GFP surface due to their similar chemical properties. Therefore, these types of monomers were prioritized in the design of GFP-targeting RHOs. There are limited examples of GFP binders due to the lack of distinct binding sites on the flat barrel surface. The only other example of increasing GFP fluorescence noncovalently—a nanobody discovered through camelid immunization—showed a 220% increase for wildtype GFP and 54% for enhanced GFP.[66] The non-covalent nanobody interaction restricts oscillations of the protein structure, limiting thermal relaxation of the chromophore

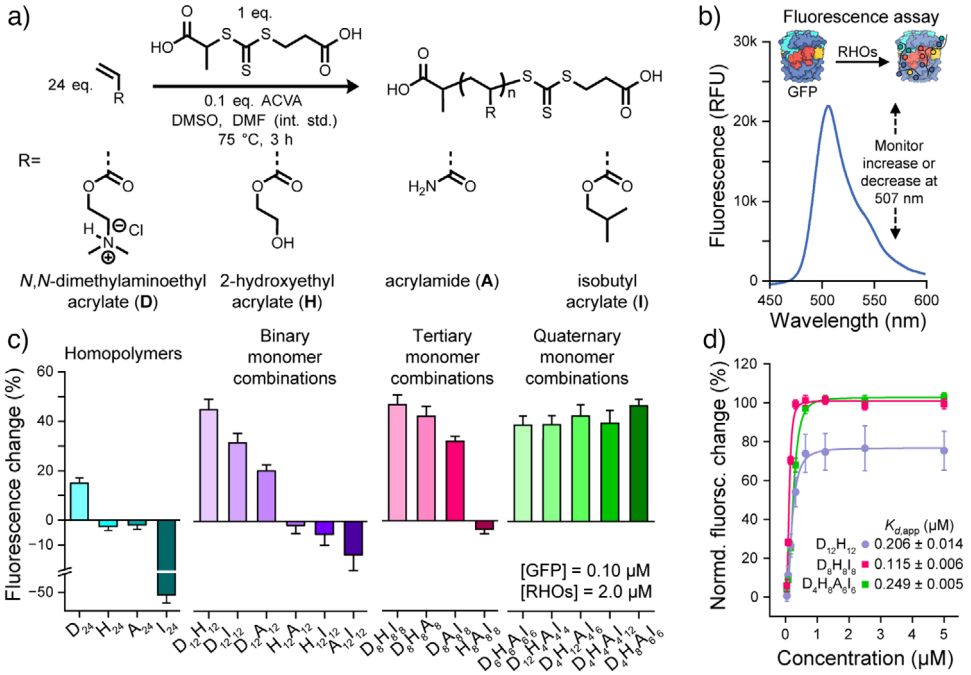

Figure 2. Description of random hetero oligomers (RHOs) and resultant fluorescence gain-of-function activity upon complexation. a) Scheme of reversible addition-fragmentation chain transfer (RAFT) polymerization of acrylates to yield RHOs, where composition is readily tuned according to input monomer stoichiometry, b) Fluorescence spectrum of green fluorescent protein (GFP) where changes in protein function were monitored at 507 nm, c) Effect of different monomer combinations and feeding ratios on GFP fluorescence in water normalized to 0% for native fluorescence, mean ± standard error, $N = 6$, d) Measured apparent dissociation constants ($K_{d,\,app}$) according to RHO composition (normalized to the fluorescence intensity of GFP–$D_4H_8A_6I_6$ as 100% fluorescence change), mean ± standard error, $N = 3$.

and increasing fluorescence as a direct readout of binding. We expect that RHOs have a similar gain-of-function effect. Therefore, GFP fluorescence changes provide a direct method to measure how RHO composition and DP affect protein binding.

Evaluation of the GFP surface (isoelectric point = 6.3) (Supplemental Information)[67] shows a large proportion of carboxylates and a net-negative surface. There are scattered hydrophobic patches and hydrogen-bond (H-bond) donors and acceptors. Combining multiple chemical properties into polymeric structures to stabilize protein surfaces is critical for RHPs.[22,24] Therefore, we used *N*,*N*-dimethylaminoethyl acrylate (DMAEA or D) and 2-(trimethylammonium)ethyl acrylate chloride to mimic positively charged amino acids (Lys, His, Arg), 2-hydroxyethyl acrylate (HEA or H) for polar amino acids (Ser and Thr), isobutyl acrylate (IBA or I) for non-polar amino acids (Leu, Val, Ile, Ala), and acrylamide (AM or A) for the polyamide backbone and amide-bearing amino acids (Gln, Asn, Figure 1). The R- and Z-groups of the chain transfer agent (CTA, R = $HOOCCHCH_3$, Z = $SSCSCH_2CH_2COOH$), acrylic acid, and 2-carboxyethyl acrylate were used to mimic anionic amino acids (Asp, Glu).

RAFT polymerizations were performed with varying monomer compositions and stoichiometries to synthesize RHOs with different chemical properties (Figure 2a). Polymerizations were run using 4,4′-azobis(4-cyanovaleric acid) at 75 °C for 3 h in DMSO. Monomer conversions reached 73%–99% by ^{1}H NMR spectroscopy (Tables S1–S4; Figures S7–S29), ensuring that overall oligomer composition corresponded to the initial monomer stoichiometry. Polymerization solutions were diluted and used in GFP binding assays in water.

GFP fluorescence was monitored at 507 nm using a 390 nm excitation wavelength and a GFP concentration of 0.10 μM (Figure 2b). Fluorescence changes were normalized to native GFP fluorescence in water. Thus, any change in fluorescence could be easily monitored. For initial analysis of how RHO composition affected GFP fluorescence, 20 × molar excess of each RHO was used (i.e., 2 μM RHO concentration in solution). Poly(*N*,*N*-dimethylaminoethyl acrylate) enhanced GFP activity by 15%, suggesting that cationic charges in RHOs led to RHOs–GFP interactions (Figure 2c). This result agrees with the cationic nature of the RHO complementing the anionic charges on the GFP surface. No activity was detected from homo-oligomers of HEA or AM. Poly(isobutyl acrylate) (PIBA) reduced the fluorescence signal, suggesting that hydrophobic RHOs denature GFP. Binary monomer copolymerizations resulted in overall enhancement of GFP fluorescence. DMAEA incorporation into RHOs always resulted in GFP fluorescence enhancement (20%–47% increases). This finding is exemplified by the increase in fluorescence (32%) observed with poly(isobutyl acrylate-co-*N*,*N*-dimethylaminoethyl acrylate) compared to PIBA, which denatured GFP.

Ternary and quaternary monomer combinations led to fluorescence increases of up to 47% over native GFP (Figure 2c), indicating that combining multiple chemical properties into RHOs leads to higher gain-of-function

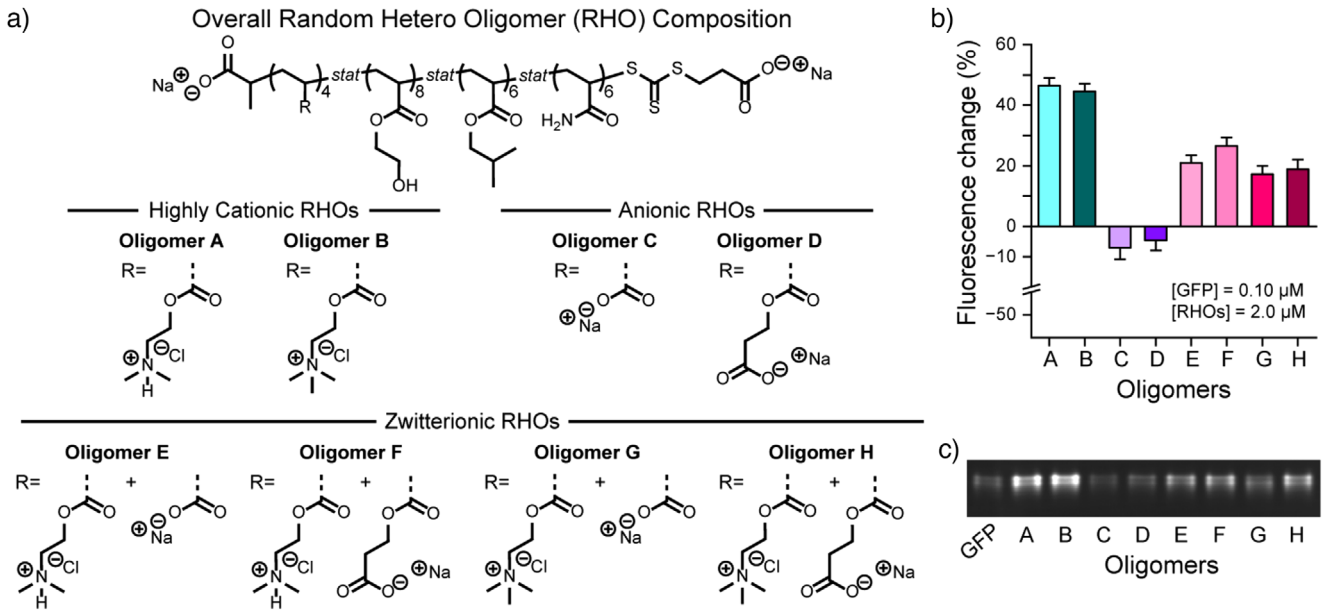

Figure 3. Random hetero oligomer (RHO) charge impacts on fluorescence changes of green fluorescent protein (GFP). a) Overall structure of RHOs and corresponding functional groups containing different identities of predominately cationic acrylates (Oligomers A and B), anionic acrylates (Oligomers C and D), and cationic and anionic acrylates (Oligomers E, F, G, H), b) GFP fluorescence changes according to RHO charge, mean ± standard error, $N = 6$, c) Native polyacrylamide gel electrophoresis image measuring GFP fluorescence according to RHO composition.

fluorescence. Reactivity ratios were measured using the Jaacks method[68] to confirm nearly-random monomer incorporation (Tables S5,S6, Figure S30). Apparent dissociation constants ($K_{d,\,app}$) were calculated for $D_{12}H_{12}$, $D_8H_8I_8$, and $D_4H_8A_6I_6$ by varying the concentration of RHOs and measuring the 50% concentration value of maximum fluorescence increase normalized to the fluorescence increase of GFP–$D_4H_8A_6I_6$ (Figure 2d). The $K_{d,\,app}$ and maximum fluorescence increases were dependent on oligomer composition, showing that while quaternary RHOs led to the highest fluorescence increase, the $K_{d,\,app}$ of tertiary RHOs was lower. These results highlight that the identity of monomers in the RHO influenced the magnitude of GFP fluorescence change, which was readily tunable according to the hydrophobic, cationic, and hydrophilic monomer content and identity.

RHOs with different ionic groups were synthesized to probe how the charge of the $D_4H_8A_6I_6$ RHO affects GFP fluorescence enhancement (Figure 3a, S31–S38, Table S7). In each polymerization, the four D monomer equivalents were substituted with either four equivalents of a different monomer or a 50:50 ratio of two monomers (i.e., two equivalents of each). To test the effect of a diffuse, permanent positive charge, we synthesized RHOs with 2-(trimethylammonium)ethyl acrylate. To test the effect of the negative charge, RHOs were synthesized with two different carboxylic acids instead of amines. To test the effect of zwitterionic RHOs, combinations of amine-containing monomers and carboxylic acid-containing monomers that ionize in neutral aqueous solutions. Swapping DMAEA with a permanently cationic monomer showed similar GFP activity enhancement (Figure 3b). When acrylic acid and 2-carboxyethyl acrylate were used, reduction of GFP fluorescence was observed. The effect of RHO ionization on GFP fluorescence was apparent during native polyacrylamide gel electrophoresis (PAGE) analysis, where different intensities of GFP fluorescence were observed even though each lane contained the same amount of GFP (Figure 3c). Given that the isoelectric point of GFP corresponds to a net anionic protein surface (pI = 6.3),[67] complementary charge matching between RHO composition and protein surface emerged as important design criteria.

Degree-Of-Polymerization Dependence Of RHOs Modulating Protein Function

We expected that degree of polymerization (DP) would impact RHO–GFP binding (Figure 4). The effect of RHO DP on GFP activity was initially investigated using RHOs with a monomer ratio of $D_1H_2I_{1.5}A_{1.5}$ and DPs of 12 and 24 (Figure 4a, Table S8). The quaternary composition was chosen for these experiments because it gave the highest fluorescence enhancement. The concentration of RHOs was tested at 0.10, 2.0, or 5.0 μM and [GFP] = 0.10 μM, corresponding to 1 ×, 20 ×, and 50 × equivalents of RHOs to GFP. RHOs of DP = 24 showed higher GFP fluorescence enhancement when compared to RHOs of DP = 12 at 0.10 and 2.0 μM. Even at a 1:1 ratio of GFP:RHO, a 12 ± 4% fluorescence increase was observed for DPs of 24. This result suggests that there are large populations of RHO compositions with strong binding interactions, contributing to the notion that sequence definition is not necessary to achieve protein recognition. Gain-of-function fluorescence saturation was observed with high concentrations of RHOs, likely because the GFP surface was saturated with RHOs. Importantly, the unpolymerized monomer control added at a concentration equal to 5.0 μM

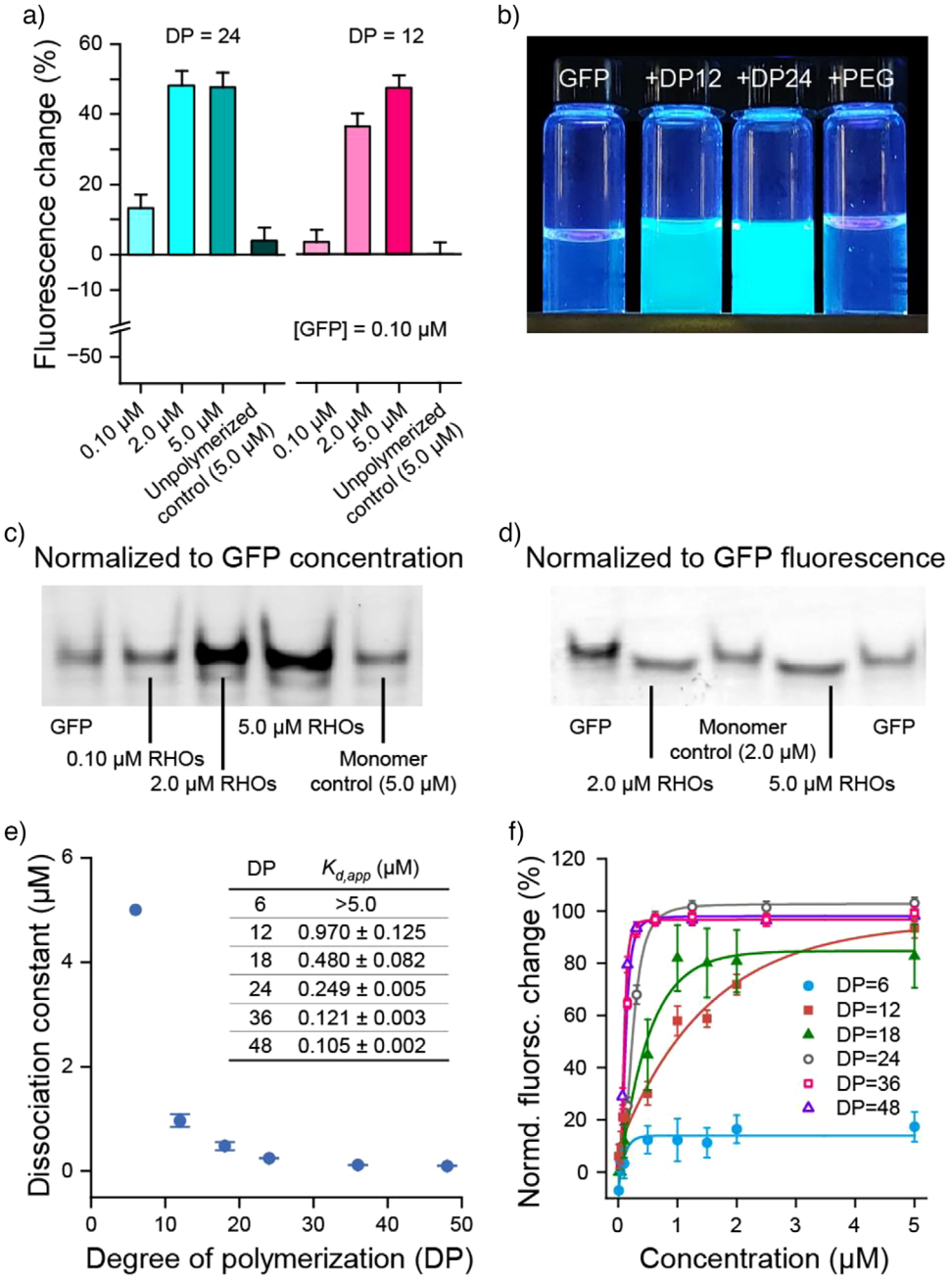

Figure 4. Effects of random hetero oligomer (RHO) degree of polymerization (DP) on green fluorescent protein (GFP) fluorescence. a) GFP fluorescence increases according to RHO DP with unpolymerized monomer controls, mean ± standard error, $N = 6$, b) Image of DP = 12 and DP = 24 RHOs visually increasing GFP fluorescence compared to 2000 g mol^{-1} poly(ethylene glycol) (PEG), c) Native polyacrylamide gel electrophoresis (PAGE) image of different concentrations of RHOs where the same amount of GFP was added to each well, d) Native PAGE where the amount of GFP added to each well was normalized to fluorescence intensity of GFP, e) Apparent dissociation constants ($K_{d,\,app}$) according to RHO DP, f) fluorescence changes of GFP according to RHO DP and composition (normalized to degree of polymerization (DP) = 24), mean ± standard error, $N = 3$.

RHOs had no significant GFP fluorescence enhancement, indicating that oligomerization is required for activity.

To test if the fluorescence increase was not a result of molecular crowding, solutions of DP = 12 or 24 mixed with GFP were compared to a solution containing 2000 g mol^{-1} poly(ethylene glycol) (PEG) and GFP (Figure 4b). Solutions showed distinct increases in brightness under UV-light irradiation compared to a solution of GFP or GFP and PEG.

Native PAGE was performed to characterize the GFP–RHO interactions. We expected to see a change in mobility upon RHO binding due to native PAGE being sensitive to both protein size and surface properties. Solutions of GFP incubated with RHOs ($D_4H_8A_6I_6$, DP = 24) showed

GFP fluorescence increases in the presence of RHOs, confirming that the RHOs–GFP complex did not dissociate under electrophoretic conditions (Figure 4c). Finally, mobility differences were visible when we reduced GFP loading to normalize fluorescence intensities (Figure 4d).

Next, DPs 6, 18, 36, and 48 were prepared to compare to DP = 12 and 24 and determine the effect of DP on the $K_{d,\,app}$ (Figures 4e, S39–S45). The $K_{d,\,app}$ was correlated to the DP of RHOs, with $K_{d,\,app}$ values decreasing (i.e., stronger binding) over 20 × when going from a DP = 6 to DP = 24 (Figure 4f). Beyond DP = 24, $K_{d,\,app}$ values moderately improved (up to 2 ×). The nanomolar $K_{d,\,app}$ values calculated for DPs 24, 36, and 48 (105–249 nM) showed that RHOs are high-affinity protein binders. However, the fluorescence increase did not change beyond DP = 24. Therefore, affinity increased with polymer DP, but gain-of-function reached a saturation point after a defined oligomer segment DP.

Privileged Protein Binders

Copolymerization of D, H, A, and I monomers results in 1 × 10^{20} oligomers that vary in length, composition, and monomer sequences according to reaction stoichiometry (Supplemental Information). A substantial amount of fluorescence enhancement likely arises from a sub-population of privileged compositions/structures/sequences with high affinity for GFP. To test this assumption, the polymerization products were fractionated by HPLC using a C-18 column to isolate 8 fractions (F1-F8), separated by increasing hydrophobicity (Figure 5a and b). Size exclusion chromatography confirmed that each fraction contained RHOs of approximately the same molar mass (Figures 5c, S47). However, ^{1}H NMR spectroscopy analysis showed that monomer composition varied between fractions (Figures 5d, S48–76, Table S9). F1 contained approximately the same amount of I and D ($D_5H_8A_5I_5$), while later fractions increased in I content and decreased in D content (e.g., F8 composition was $D_2H_7A_5I_8$). The A and H content remained approximately the same between the fractions.

To examine how minor changes in charge and hydrophobicity across RHO fractions affected GFP fluorescence, the concentrations of F1-F8 were normalized using the CTA absorbance at 309 nm. We incubated these solutions with 0.10 μM GFP, then measured fluorescence. Fractions showed different activity when tested at 0.25 and 2.0 μM RHOs (i.e., 2.5 × and 20 × equivalents relative to GFP). Fractions that contained approximately equal amounts of D and I (i.e., F1, $D_5H_8A_5I_5$) showed higher fluorescence enhancement (100 ± 9% for 2.0 μM RHOs) compared to fractions that contained more I (i.e., F8, $D_2H_7A_5I_8$, 73 ± 9% for 2.0 μM RHOs, Figure 5e). The experiments conducted at 0.25 μM RHOs showed that the fluorescence enhancement of GFP in the presence of $D_5H_8A_5I_5$ (F1) was ~98% of the fluorescence enhancement compared to the experiments using 2.0 μM of the same RHO. In contrast to $D_5H_8A_5I_5$ (F1), $D_2H_7A_5I_8$ (F8) only showed a 29% fluorescence enhancement at 0.25 μM RHOs compared to experiments using 2.0 μM of the same RHO. These experiments suggest differences between $K_{d,\,app}$ values according to RHO compositions fractionated via HPLC. Relative to the polymerization products (0.83 ± 0.06 μM) (Figure 5f), a two-fold decrease in $K_{d,\,app}$ was observed for F1 (0.34 ± 0.03 μM). Conversely, a three-fold increase in $K_{d,\,app}$ compared to the polymerization solution was observed for F8 (2.2 ± 0.5 μM). These data suggested that $K_{d,\,app}$ values of RHOs can vary >6.5 × within a single polymerization product, highlighting that sub-populations can be isolated that show substantially higher binding affinity for GFP.

Characterizing RHO–Protein Binding

The $K_{d,\,app}$ values from fluorescence assays are a relative measure of the RHO–GFP interaction strength. Using native PAGE, the $D_5H_8A_5I_5$(F1)–GFP complex showed more pronounced mobility differences compared to the $D_2H_7A_5I_8$(F8)–GFP complex and GFP alone (Figure 6a). These results suggest that the stronger-binding $D_5H_8A_5I_5$ (F1) RHOs modify the surface properties of GFP.

We used dynamic light scattering (DLS) analysis to measure if RHO–GFP complexation led to an increased hydrodynamic diameter (Figure 6b). We removed unbound RHOs (i.e., weakly binding oligomers) via spin filtration (15 kDa MWCO) to ensure that only RHO–GFP complexes were present during size measurements. UV-Vis spectroscopy was used to calculate a molar ratio of RHOs and GFP after purification using the characteristic absorption of the CTA thiocarbonylthio (309 nm) and GFP (465 nm). RHO $D_5H_8A_5I_5$ (F1) showed a ratio of 6.8 RHOs to 1 GFP and $D_2H_7A_5I_8$ (F8) showed a ratio of 2.4 RHOs to 1 GFP (Figure S77). Complexation between the RHOs and GFP depended on oligomer composition since the $D_5H_8A_5I_5$(F1)–GFP sample yielded a larger hydrodynamic diameter (10.3 ± 0.2 nm) compared to GFP (6.6 ± 0.2 nm) and $D_2H_7A_5I_8$(F8)–GFP (6.6 ± 0.1 nm) (Figure 6b).

Zeta potential analysis was used to measure the surface charge of RHO–GFP complexes. The zeta potential of $D_5H_8A_5I_5$(F1)–GFP complex was –0.55 mV compared to –9.1 mV for GFP and –7.7 mV for $D_2H_7A_5I_8$(F8)–GFP (Figure 6b). The minimal negative surface charge detected for the $D_5H_8A_5I_5$(F1)–GFP complex is consistent with the high D content of the RHO binding to the anionic surface of the protein. The minor change in surface charge for $D_2H_7A_5I_8$(F8)–GFP suggested minor RHO–protein complexation, reflecting a lower affinity for GFP compared to $D_5H_8A_5I_5$ (F1).

To obtain a quantitative K_d value among RHOs and GFP, we performed microscale thermophoresis (MST) measurements.[69] We expected RHO–GFP complexes to diffuse differently compared to GFP under a thermal gradient. GFP diffusion was monitored at different concentrations of RHOs (either polymerization products, $D_5H_8A_5I_5$, or $D_2H_7A_5I_8$) (Figure 6c). The thermophoresis detected for $D_5H_8A_5I_5$(F1)–GFP (0.20-1.80 μM RHOs; [GFP] = 0.30 μM) can be approximated by a sigmoidal binding model, yielding a K_d = 0.89 ± 0.06 μM. This K_d value is comparable with fluorescence assays that determined the $K_{d,\,app}$ (0.34 ± 0.03 μM). The thermophoresis measurements

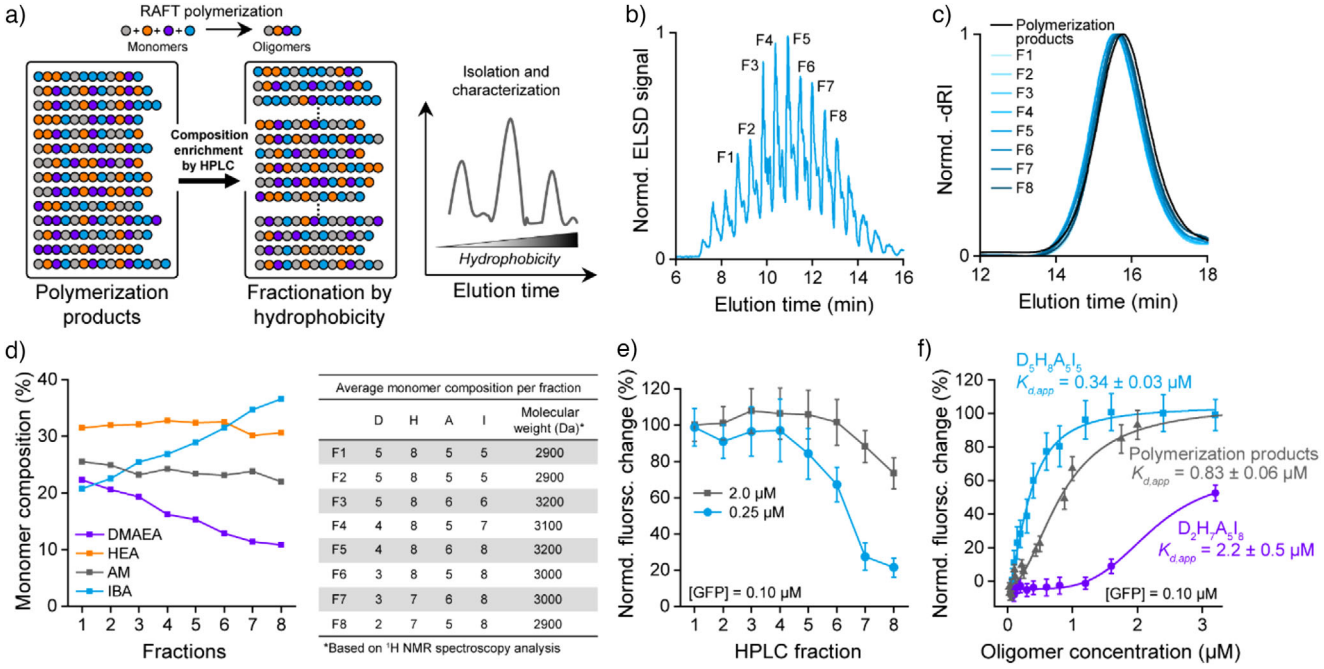

Figure 5. Isolation and characterization of privileged RHOs. a) Scheme representing fraction of the polymerization products using HPLC. b) Chromatogram of the evaporative light scattering detector (ELSD) response during preparative HPLC using a C-18 column to fractionate the RAFT polymerization products. c) Size exclusion chromatography of HPLC fractions showed that the fractions had nearly identical molar mass distributions. d) Monomer composition analysis using ^{1}H NMR spectroscopy of HPLC elution fractions, e) Fluorescence enhancement of different HPLC fractions at 0.25 and 2.0 μM in water (normalized to the saturated fluorescence enhancement for HPLC fraction 1 at 2.0 μM RHO), mean ± standard error, $N = 3$, f) Determination of apparent dissociation constant for $D_5H_8A_5I_5$ (F1) and $D_2H_7A_5I_8$ (F8) compositionally enriched RHOs in water, mean ± standard error, $N = 3$.

analyzing the polymerization products or $D_2H_7A_5I_8$ fit a non-binding model, suggesting weaker oligomer-protein interactions than $D_5H_8A_5I_5$(F1)–GFP.

RHOs binding to the GFP surface likely compete with intra-protein interactions, which may influence GFP stability when heated. To determine if $D_5H_8A_5I_5$ (F1) stabilized or destabilized GFP, variable temperature circular dichroism spectroscopy was used to monitor the secondary structure of GFP (Figure 6d). The melting temperature of GFP was reduced from 63.1°C to 59.1 °C in the presence of $D_5H_8A_5I_5$ (F1). While this result seems to contradict the increase in GFP fluorescence, GFP nanobodies that bind at nanomolar concentrations also decreased the melting temperature of GFP.[70] We expect that at lower temperatures, the RHOs restrict oscillations of the protein structure, limiting some thermal relaxation of the chromophore. As the temperature increases, the amphiphilicity of the RHOs becomes deleterious and denatures the protein.

To identify the specificity of $D_5H_8A_5I_5$(F1)–GFP and $D_2H_7A_5I_8$(F8)–GFP interactions, we added RHOs to GFP in the presence of bovine serum album (BSA). BSA was used as a molecular crowding agent and a potential RHO binding competitor versus GFP since BSA has a more negative surface charge (pI = 4.7 for BSA vs. pI = 6.3 for GFP) and is significantly larger (66 kDa)[71] than GFP (31 kDa). If only charge–charge interactions dominate RHO–GFP interactions, we would expect partitioning of the RHOs to BSA. Three solutions were set up with: 1) BSA and GFP, 2) RHOs and GFP, or 3) BSA, GFP, and RHOs. These solutions were incubated for 24 h. Subsequently, BSA was added to the RHO–GFP solution and RHOs were added to the BSA–GFP solution. All three solutions were incubated for an additional 24 h, then measured for GFP fluorescence. These binding competition experiments revealed that $D_5H_8A_5I_5$ (F1) oligomers had higher affinity for GFP compared to BSA (Figure 6e) because an unchanged GFP fluorescence increase was observed until 10-fold BSA to RHO was present, when a minor decrease in fluorescence was observed. Conversely, the low binding RHO composition $D_2H_7A_5I_8$ (F8) showed cooperative fluorescence enhancement as BSA concentration increased, suggesting competing or interdependent GFP and BSA binding. This straightforward competition assay suggests that overall composition, instead of only charge–charge interactions, lead to more selective and stronger-binding RHOs.

We conducted well-tempered metadynamics (WTMD) simulations[72] to construct binding free energy landscapes over the cylindrical surface of the GFP β-barrel (Tables S10,S11, Figures S79–S82) for randomly generated sequences of $D_5H_8A_5I_5$ (F1, Figure 7a) and $D_2H_7A_5I_8$ (F8, Figure 7b), to compare to poly(ethylene glycol) (PEG) oligomers in complex with GFP (Figure S90).[73–77] All three oligomers exhibited favorable binding to GFP but showed distinct free energy topographies (Table S12, Figures S83–S90). PEG oligomer showed shallow and spatially confined minima, primarily concentrated atop the GFP β-barrel (Figure S90), indicative

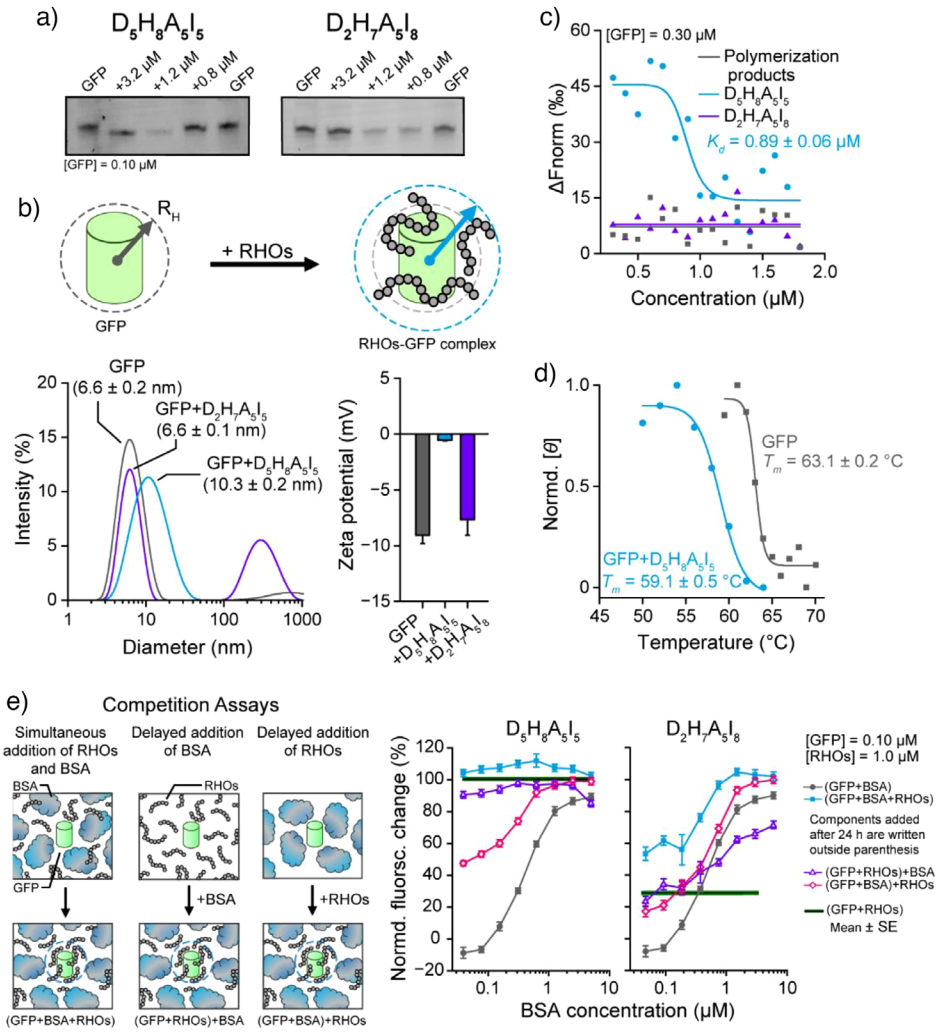

Figure 6. Binding studies analyzing random hetero oligomer (RHO) interactions with green fluorescent protein (GFP). a) Detection of mobility differences of RHO–GFP complexes by native polyacrylamide gel electrophoresis with strong-binding $D_5H_8A_5I_5$ (F1) and $D_2H_7A_5I_8$ (F8), b) Visualization of RHO–GFP interactions and detection of complex formation through hydrodynamic size increase (mean of four replicates) and zeta potential (mean of three replicates) neutralization using dynamic light scattering analysis, c) Microscale thermophoresis analysis of RHO–GFP complex formation, d) Determination of melting temperature of GFP with and without $D_5H_8A_5I_5$ oligomers in water using variable temperature circular dichroism spectroscopy (data at 233 nm were used to calculate T_m values), e) Competition assays using bovine serum albumin (BSA) measured after 48 h incubation in water, where different concentrations of BSA were added to RHOs and GFP at different points of incubation: (GFP + BSA + RHOs) is all components added at the beginning of the assay, (GFP + RHOs)+BSA is an assay where BSA was added 24 h after initial incubation of GFP and RHOs, (GFP + BSA)+RHOs is an assay where RHOs were added 24 h after initial incubation of GFP and BSA, (GFP + BSA) and (GFP + RHOs) are controls to measure the separate bimolecular interactions, mean ± standard error, $N = 3$.

of weak and nonspecific interactions. $D_5H_8A_5I_5$ (F1) yielded a rugged free energy surface characterized by six (6) deep minima distributed across the β-barrel (Figure 7a), showing several low-energy stable binding configurations with extended conformations across the GFP barrel (Figure 7c). This topographic breadth suggests a promiscuous binding mode and may be associated with stronger interaction energies and longer residence times, facilitated by multiple metastable states that reduce the likelihood of rapid dissociation. This number of strong binding sites correlates with the measured 6.8 RHOs per GFP during DLS analysis (Figure S77). The $D_2H_7A_5I_8$ (F8) oligomer showed a more constrained landscape with two to three localized wells (Figure 7b), indicating a spatially restricted binding interface with less binding area across the barrel (Figure 7d). This limited configurational flexibility correlates with shorter residence times, more transient interactions, and the number of RHOs measured during DLS analysis (2.4 RHO per GFP, Figure S77). These WTMD results suggest that while most RHO oligomer compositions from a RAFT polymerization likely bind GFP to some extent, the strength, persistence, and area of binding on the surface on GFP are dependent on specific oligomer composition.

Molecular dynamics (MD) simulations with the polarizable AMOEBA force field were run to analyze the RHO–GFP complexes (Figures S92,S93) predicted by WTMD.[78] After the simulations, we computed the total interaction energy (IE) between each monomer and GFP as the sum of van der Waals, permanent, and induced electrostatics (Figures

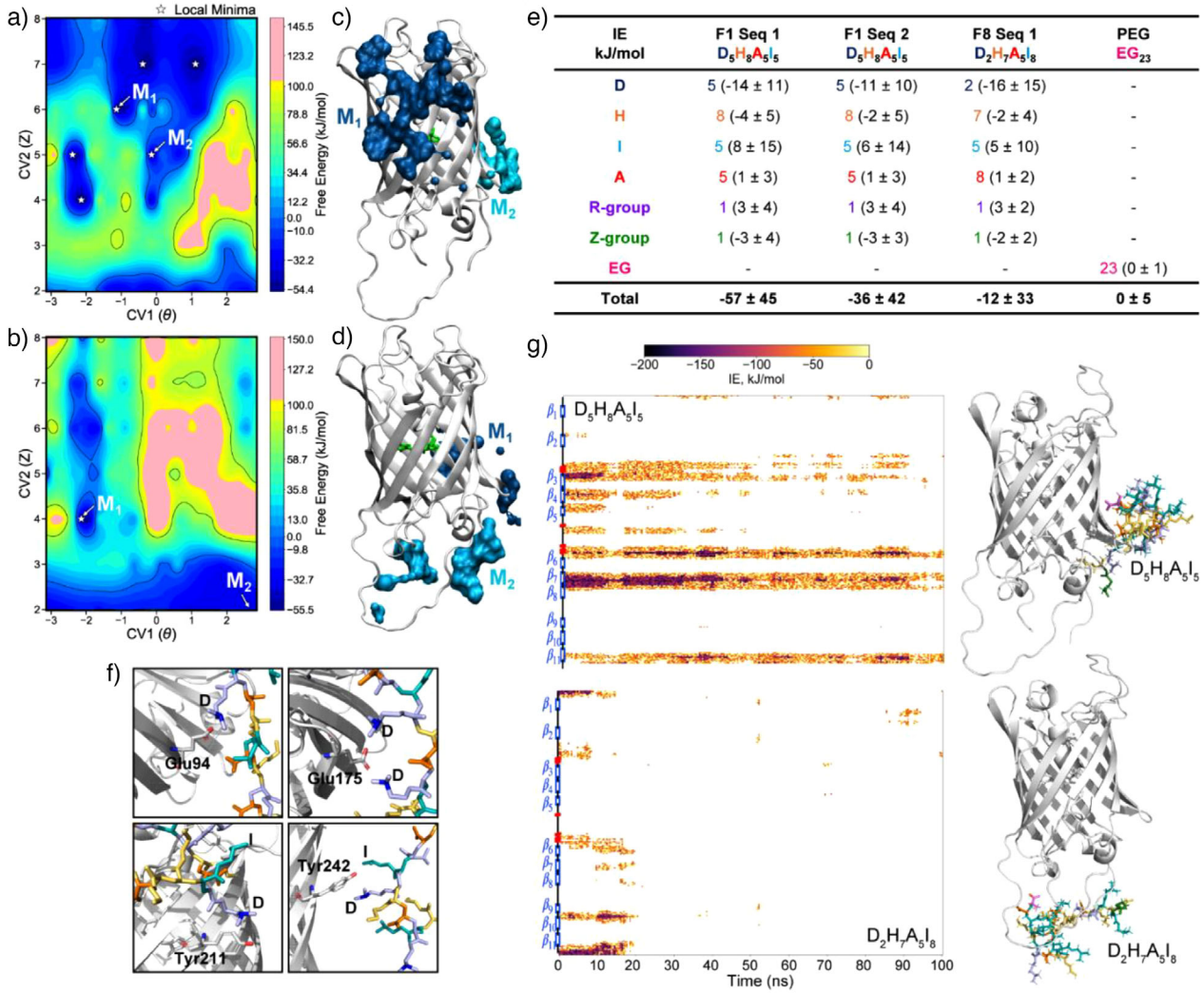

IE kJ/mol	F1 Seq 1 $D_5H_8A_5I_5$	F1 Seq 2 $D_5H_8A_5I_5$	F8 Seq 1 $D_2H_7A_5I_8$	PEG EG_{23}
D	5 (-14 ± 11)	5 (-11 ± 10)	2 (-16 ± 15)	-
H	8 (-4 ± 5)	8 (-2 ± 5)	7 (-2 ± 4)	-
I	5 (8 ± 15)	5 (6 ± 14)	5 (5 ± 10)	-
A	5 (1 ± 3)	5 (1 ± 3)	8 (1 ± 2)	-
R-group	1 (3 ± 4)	1 (3 ± 4)	1 (3 ± 2)	-
Z-group	1 (-3 ± 4)	1 (-3 ± 3)	1 (-2 ± 2)	-
EG	-	-	-	23 (0 ± 1)
Total	**-57 ± 45**	**-36 ± 42**	**-12 ± 33**	**0 ± 5**

Figure 7. Computational characterization of random hetero oligomer (RHO)–green fluorescent protein (GFP) interactions. a) Normalized free energy surface for the $D_5H_8A_5I_5$ (F1) oligomer with multiple low-energy minima shown with white arrows on the GFP surface, b) Normalized free energy surface for the $D_2H_7A_5I_8$ (F8) oligomer with multiple low-energy minima shown with white arrows on the GFP surface, c) The regions on GFP protein highlighted in blue and cyan surface colors show oligomer binding locations for two energy minima shown as M1 and M2 in (a) for the $D_5H_8A_5I_5$ (F1) oligomer, d) The regions on GFP protein highlighted in blue and cyan surface colors show oligomer binding locations for two energy minima shown as M1 and M2 in (c) for the $D_2H_7A_5I_8$ (F8) oligomer, e) Total interaction energies (IE) between oligomers and GFP, f) Representative molecular zoomed in snapshots showing the strongest monomer (D)-GFP interactions for F1 oligomers, g) IEs over the course of the MD simulation for $D_5H_8A_5I_5$ (F1) Seq 1 (top) and $D_2H_7A_5I_8$ (F8) Seq 1 (bottom). Representative snapshots are shown to illustrate the relative position of the oligomer with respect to GFP in each case.

S94,S95). IE is most favorable for $D_5H_8A_5I_5$ (F1) Seq 1, followed by $D_5H_8A_5I_5$ (F1) Seq 2, then $D_2H_7A_5I_8$ (F8) Seq 1 (Figure 7e), further suggesting that overall composition governs RHO–GFP interactions. The decomposition of IE into contributions from individual monomers indicates that D is the strongest binder, interacting with primarily Glu and Tyr residues in GFP (Figure 7f). Our MD simulations show that $D_5H_8A_5I_5$ (F1) Seq 1 RHOs bind across the β-barrel and that the contacts are preserved throughout our 100 ns simulations (Figures 7g, S96–S101). Meanwhile, the weakest binding RHO, $D_2H_7A_5I_8$ (F8) Seq 1, interacts with the unstructured loops at the bottom of the barrel for only a fraction of the time (27 ns). Residence times of the other RHOs in the vicinity of GFP follow the energy trends (Figure S102). These simulations further confirm that the compositional variance from a single RAFT polymerization results in RHOs with different binding interactions and strengths, which can be successfully isolated and analyzed using multiple analytical and computational approaches.

Conclusion

Molecular definition is usually a pre-requisite for protein recognition and functional modulation. Even polymeric scaffolds that yield protein specificity (molecularly imprinted polymers),[79,80] rely on molecular pre-arrangement around the protein target prior to polymerization. In this report,

we show that oligomers can be rationally designed based on key information about the protein surface. Complementary charge and length matching with the protein surface were critical to achieving nanomolar binding interactions with saturation of gain-of-function. Future work into the segmental location of monomers within RHOs will provide further insight into the impact of random versus semi-controlled monomer sequences.

Straightforward purification of the polymerization via HPLC isolated privileged RHO binders from weaker or non-binding RHOs with dissociation constants varying >6.5 ×. These results were confirmed via two different computational approaches to visualize how a few randomly generated sequences interacted with GFP. Monte Carlo simulations were used to estimate the fraction of synthesized oligomers that showed high affinity for GFP (Figures S96,S103). Approximately 5.0% of the simulated compositions were predicted to have >95% compositional similarity to the high-performing RHO $D_5H_8A_5I_5$ (Figure S104). Given that 6 to 7 $D_5H_8A_5I_5$ oligomers were observed to bind to GFP experimentally at a 20-fold excess, then at least 30%–35% of the 5.0% of $D_5H_8A_5I_5$ RHOs would be binding to GFP. This corresponds to at least 1.5% of the total oligomers resulting from the RAFT polymerization (or 1.5×10^{18} different sequences) complexing with GFP. This expansive sequence variance of binders from a single polymerization introduces an opportunity to further isolate and identify strong and selective RHOs for proteins with no apparent binding sites, particularly if monomer reactivity ratios are leveraged to control polymer sequences.[68] We expect that methods to more discretely control polyacrylate structure[81–90] paired with advanced purification[91–95] to separate compositional sub-populations will assist in approaching low nanomolar/picomolar dissociation constants and further protein selectivity.

Overall, these results show that polyacrylates with defined monomer compositions, but random sequences, can achieve protein recognition and allosteric regulation for next-generation sensing, therapeutic, responsive, and/or catalytic materials. A few examples of these materials may include enhancing antibody performance in point-of-care diagnostics, selective protein purification or precipitation during production, or as standalone diagnostic materials. In the long term, this approach has the potential to be a high-throughput protocol to develop therapeutically relevant biological binders akin to phage display[96] or SELEX,[97] but with the scalability of acrylic materials.

Supporting Information

The authors have cited additional references within the Supporting Information.[98-122]

Acknowledgements

The authors acknowledge J. Matson, R. Gandour, and B. Sumerlin for helpful discussions. The authors also thank the Advanced Research Computing center at Virginia Tech for providing computational resources and technical support that have contributed to the results reported within this study. The authors gratefully acknowledge financial support from startup funds from the Department of Chemistry at Virginia Tech. This work was supported by the National Institute of Health, National Institute of General Medical Sciences, under award number R35-GM150409 for financial support. This work was supported by GlycoMIP, a National Science Foundation (NSF) Materials Innovation Platform (MIP) funded through Cooperative Agreement DMR-1933525.

Conflict of Interests

The authors declare no conflict of interest.

Data Availability Statement

The data that support the findings of this study are available from the corresponding author upon reasonable request.

Keywords: Copolymers · Polymer synthesis · Polymer–protein conjugate · Protein · RAFT

[1] G. Schreiber, A. E. Keating, *Curr. Opin. Struct. Biol.* **2011**, *21*, 50–61, https://doi.org/10.1016/j.sbi.2010.10.002.
[2] E. Ostuni, B. A. Grzybowski, M. Mrksich, C. S. Roberts, G. M. Whitesides, *Langmuir* **2003**, *19*, 1861–1872.
[3] M. Tanada, M. Tamiya, A. Matsuo, A. Chiyoda, K. Takano, T. Ito, M. Irie, T. Kotake, R. Takeyama, H. Kawada, R. Hayashi, S. Ishikawa, K. Nomura, N. Furuichi, Y. Morita, M. Kage, S. Hashimoto, K. Nii, H. Sase, K. Ohara, A. Ohta, S. Kuramoto, Y. Nishimura, H. Iikura, T. Shiraishi, *J. Am. Chem. Soc.* **2023**, *145*, 16610–16620, https://doi.org/10.1021/jacs.3c03886.
[4] A. K. Arya, A. El-Fert, T. Devling, R. M. Eccles, M. A. Aslam, C. P. Rubbi, N. Vlatković, J. Fenwick, B. H. Lloyd, D. R. Sibson, T. M. Jones, M. T. Boyd, *Br. J. Cancer* **2010**, *103*, 186–195, https://doi.org/10.1038/sj.bjc.6605739.
[5] S. Vázquez Torres, M. Benard Valle, S. P. Mackessy, S. K. Menzies, N. R. Casewell, S. Ahmadi, N. J. Burlet, E. Muratspahić, I. Sappington, M. D. Overath, E. Rivera-de-Torre, J. Ledergerber, A. H. Laustsen, K. Boddum, A. K. Bera, A. Kang, E. Brackenbrough, I. A. Cardoso, E. P. Crittenden, R. J. Edge, J. Decarreau, R. J. Ragotte, A. S. Pillai, M. Abedi, H. L. Han, S. R. Gerben, A. Murray, R. Skotheim, L. Stuart, L. Stewart, T. J. A. Fryer, T. P. Jenkins, D. Baker, *Nature* **2025**, *639*, 225–231, https://doi.org/10.1038/s41586-024-08393-x.
[6] R. Rohs, S. M. West, A. Sosinsky, P. Liu, R. S. Mann, B. Honig, *Nature* **2009**, *461*, 1248–1253, https://doi.org/10.1038/nature08473.
[7] K. L. Hudson, G. J. Bartlett, R. C. Diehl, J. Agirre, T. Gallagher, L. L. Kiessling, D. N. Woolfson, *J. Am. Chem. Soc.* **2015**, *137*, 15152–15160, https://doi.org/10.1021/jacs.5b08424.
[8] H. Kaur, J. G. Bruno, A. Kumar, T. K. Sharma, *Theranostics* **2018**, *8*, 4016–4032, https://doi.org/10.7150/thno.25958.
[9] P. H. Winegar, C. A. Figg, M. H. Teplensky, N. Ramani, C. A. Mirkin, *Chem* **2022**, *8*, 3018–3030.
[10] K. M. Herbert, S. Schrettl, S. J. Rowan, C. Weder, *Macromolecules* **2017**, *50*, 8845–8870, https://doi.org/10.1021/acs.macromol.7b01607.

[11] T. P. Russell, Y. Chai, *Macromolecules* **2017**, *50*, 4597–4609, https://doi.org/10.1021/acs.macromol.7b00418.

[12] S. K. Kumar, B. C. Benicewicz, R. A. Vaia, K. I. Winey, *Macromolecules* **2017**, *50*, 714–731, https://doi.org/10.1021/acs.macromol.6b02330.

[13] D. K. Schneiderman, M. A. Hillmyer, *Macromolecules* **2017**, *50*, 3733–3749, https://doi.org/10.1021/acs.macromol.7b00293.

[14] J. G. H. Hermens, T. Freese, K. J. van den Berg, R. van Gemert, B. L. Feringa, *Sci. Adv.* **2020**, *6*, eabe0026.

[15] J.-F. Lutz, M. Ouchi, D. R. Liu, M. Sawamoto, *Science* **2013**, *341*, 1238149, https://doi.org/10.1126/science.1238149.

[16] J.-F. Lutz, *Eur. Polym. J.* **2023**, *199*, 112465, https://doi.org/10.1016/j.eurpolymj.2023.112465.

[17] C. Yang, K. B. Wu, Y. Deng, J. Yuan, J. Niu, *ACS Macro Lett.* **2021**, *10*, 243–257.

[18] M. R. Arkin, J. A. Wells, *Nat. Rev. Drug Discovery* **2004**, *3*, 301–317, https://doi.org/10.1038/nrd1343.

[19] K. Wu, H. Bai, Y.-T. Chang, R. Redler, K. E. McNally, W. Sheffler, T. J. Brunette, D. R. Hicks, T. E. Morgan, T. J. Stevens, A. Broerman, I. Goreshnik, M. DeWitt, C. M. Chow, Y. Shen, L. Stewart, E. Derivery, D. A. Silva, G. Bhabha, D. C. Ekiert, D. Baker, *Nature* **2023**, *616*, 581–589, https://doi.org/10.1038/s41586-023-05909-9.

[20] H. Lee, T. Xie, B. Kang, X. Yu, S. W. Schaffter, R. Schulman, *Nat. Commun.* **2024**, *15*, 7973, https://doi.org/10.1038/s41467-024-51907-4.

[21] R.-M. Lu, Y.-C. Hwang, I.-J. Liu, C.-C. Lee, H.-Z. Tsai, H.-J. Li, H.-C. Wu, *J. Biomed. Sci.* **2020**, *27*, 1, https://doi.org/10.1186/s12929-019-0592-z.

[22] B. Panganiban, B. Qiao, T. Jiang, C. DelRe, M. M. Obadia, T. D. Nguyen, A. A. A. Smith, A. Hall, I. Sit, M. G. Crosby, P. B. Dennis, E. Drockenmuller, M. Olvera de la Cruz, T. Xu, *Science* **2018**, *359*, 1239–1243, https://doi.org/10.1126/science.aao0335.

[23] H. Koide, C. Kiyokawa, A. Okishima, K. Saito, K. Yoshimatsu, T. Fukuta, Y. Hoshino, T. Asai, Y. Nishimura, Y. Miura, N. Oku, K. J. Shea, *J. Am. Chem. Soc.* **2023**, *145*, 23143–23151, https://doi.org/10.1021/jacs.3c06799.

[24] I. Jayapurna, Z. Ruan, M. Eres, P. Jalagam, S. Jenkins, T. Xu, *Biomacromolecules* **2023**, *24*, 652–660, https://doi.org/10.1021/acs.biomac.2c01036.

[25] Z. Ruan, S. Li, A. Grigoropoulos, H. Amiri, S. L. Hilburg, H. Chen, I. Jayapurna, T. Jiang, Z. Gu, A. Alexander-Katz, C. Bustamante, H. Huang, T. Xu, *Nature* **2023**, *615*, 251–258, https://doi.org/10.1038/s41586-022-05675-0.

[26] M. A. Sanders, S. S. Chittari, J. R. Foley, W. M. Swofford, B. M. Elder, A. S. Knight, *J. Am. Chem. Soc.* **2024**, *146*, 17404–17413, https://doi.org/10.1021/jacs.4c05040.

[27] H. Rothfuss, N. D. Knöfel, P. W. Roesky, C. Barner-Kowollik, *J. Am. Chem. Soc.* **2018**, *140*, 5875–5881, https://doi.org/10.1021/jacs.8b02135.

[28] Y. Liu, S. Pujals, P. J. M. Stals, T. Paulöhrl, S. I. Presolski, E. W. Meijer, L. Albertazzi, A. R. A. Palmans, *J. Am. Chem. Soc.* **2018**, *140*, 3423–3433, https://doi.org/10.1021/jacs.8b00122.

[29] Y. Müllers, A. S. Sadr, M. Schenderlein, N. Pallab, M. D. Davari, U. Glebe, M. Reifarth, *ChemCatChem* **2024**, *16*, e202301685.

[30] M. Xie, X. Jia, X. Xu, *Phys. Chem. Chem. Phys.* **2024**, *26*, 4052–4061, https://doi.org/10.1039/D3CP05017C.

[31] J. Walkowiak, Y. Lu, M. Gradzielski, S. Zauscher, M. Ballauff, *Macromol. Rapid Commun.* **2020**, *41*, 1900421, https://doi.org/10.1002/marc.201900421.

[32] V. Guerlavais, T. K. Sawyer, L. Carvajal, Y. S. Chang, B. Graves, J.-G. Ren, D. Sutton, K. A. Olson, K. Packman, K. Darlak, C. Elkin, E. Feyfant, K. Kesavan, P. Gangurde, L. T. Vassilev, H. M. Nash, V. Vukovic, M. Aivado, D. A. Annis, *J. Med. Chem.* **2023**, *66*, 9401–9417, https://doi.org/10.1021/acs.jmedchem.3c00623.

[33] P. Sang, Z. Zhou, Y. Shi, C. Lee, Z. Amso, D. Huang, T. Odom, V. T. B. Nguyen-Tran, W. Shen, J. Cai, *Sci. Adv.* **2023**, *6*, eaaz4988.

[34] S. Muyldermans, T. N. Baral, V. C. Retamozzo, P. De Baetselier, E. De Genst, J. Kinne, H. Leonhardt, S. Magez, V. K. Nguyen, H. Revets, U. Rothbauer, B. Stijlemans, S. Tillib, U. Wernery, L. Wyns, Gh. Hassanzadeh-Ghassabeh, D. Saerens, *Vet. Immunol. Immunopathol.* **2009**, *128*, 178–183, https://doi.org/10.1016/j.vetimm.2008.10.299.

[35] J. Bethuyne, S. De Gieter, O. Zwaenepoel, A. Garcia-Pino, K. Durinck, A. Verhelle, G. Hassanzadeh-Ghassabeh, F. Speleman, R. Loris, J. Gettemans, *Nucleic. Acids. Res.* **2014**, *42*, 12928–12938, https://doi.org/10.1093/nar/gku962.

[36] M. Liu, C. Li, M. Pazgier, C. Li, Y. Mao, Y. Lv, B. Gu, G. Wei, W. Yuan, C. Zhan, W.-Y. Lu, W. Lu, *Proc. Natl. Acad. Sci. USA* **2010**, *107*, 14321–14326, https://doi.org/10.1073/pnas.1008930107.

[37] P. Sang, Y. Shi, J. Lu, L. Chen, L. Yang, W. Borcherds, S. Abdulkadir, Q. Li, G. Daughdrill, J. Chen, J. Cai, *J. Med. Chem.* **2020**, *63*, 975–986, https://doi.org/10.1021/acs.jmedchem.9b00993.

[38] P. Sang, J. Cai, *Chem. Soc. Rev.* **2023**, *52*, 4843–4877.

[39] T. Hara, S. R. Durell, M. C. Myers, D. H. Appella, *J. Am. Chem. Soc.* **2006**, *128*, 1995–2004, https://doi.org/10.1021/ja056344c.

[40] T. Kamura, Y. Katsuda, Y. Fuchigami, Y. Itsuki, Y. Kitamura, T. Sakurai, T. Ozawa, T. Ihara, *Bull. Chem. Soc. Jpn.* **2023**, *96*, 241–246, https://doi.org/10.1246/bcsj.20220331.

[41] Y. Liu, L. Wang, H. Li, L. Zhao, Y. Ma, Y. Zhang, J. Liu, Y. Wei, *Prog. Polym. Sci.* **2024**, *150*, 101790, https://doi.org/10.1016/j.progpolymsci.2024.101790.

[42] J. Gao, S. Le, S. Thayumanavan, *Angew. Chem. Int. Ed.* **2021**, *133*, 27395–27400, https://doi.org/10.1002/ange.202109477.

[43] A. P. Blum, J. K. Kammeyer, J. Yin, D. T. Crystal, A. M. Rush, M. K. Gilson, N. C. Gianneschi, *J. Am. Chem. Soc.* **2014**, *136*, 15422–15437, https://doi.org/10.1021/ja5088216.

[44] K. P. Carrow, H. L. Hamilton, M. P. Hopps, Y. Li, B. Qiao, N. C. Payne, M. P. Thompson, X. Zhang, A. Magassa, M. Fattah, S. Agarwal, M. P. Vincent, M. Buyanova, P. A. Bertin, R. Mazitschek, M. Olvera de la Cruz, D. A. Johnson, J. A. Johnson, N. C. Gianneschi, *Adv. Mater.* **2024**, *36*, 2311467, https://doi.org/10.1002/adma.202311467.

[45] S. P. Le, J. Krishna, P. Gupta, R. Dutta, S. Li, J. Chen, S. Thayumanavan, *Biomacromolecules* **2024**, *25*, 6229–6249, https://doi.org/10.1021/acs.biomac.4c00850.

[46] C. Renner, J. Piehler, T. Schrader, *J. Am. Chem. Soc.* **2006**, *128*, 620–628, https://doi.org/10.1021/ja0560229.

[47] B. S. Sandanaraj, R. Demont, S. V. Aathimanikandan, E. N. Savariar, S. Thayumanavan, *J. Am. Chem. Soc.* **2006**, *128*, 10686–10687, https://doi.org/10.1021/ja063544v.

[48] S. J. Koch, C. Renner, X. Xie, T. Schrader, *Angew. Chem. Int. Ed.* **2006**, *45*, 6352–6355, https://doi.org/10.1002/anie.200601161.

[49] B. S. Sandanaraj, D. R. Vutukuri, J. M. Simard, A. Klaikherd, R. Hong, V. M. Rotello, S. Thayumanavan, *J. Am. Chem. Soc.* **2005**, *127*, 10693–10698, https://doi.org/10.1021/ja051947+.

[50] G. Wu, T. Jin, A. Alexander-Katz, C. W. Coley, *Matter* **2025**, 102336.

[51] M. J. Tamasi, R. A. Patel, C. H. Borca, S. Kosuri, H. Mugnier, R. Upadhya, N. S. Murthy, M. A. Webb, A. J. Gormley, *Adv. Mater.* **2022**, *34*, 2201809, https://doi.org/10.1002/adma.202201809.

[52] T. Jiang, A. Hall, M. Eres, Z. Hemmatian, B. Qiao, Y. Zhou, Z. Ruan, A. D. Couse, W. T. Heller, H. Huang, M. O. de la Cruz, M. Rolandi, T. Xu, *Nature* **2020**, *577*, 216–220, https://doi.org/10.1038/s41586-019-1881-0.

[53] K. M. M. Messina, A. M. Woys, *Pharm. Res.* **2023**, *40*, 525–536, https://doi.org/10.1007/s11095-022-03436-2.

[54] C. Bapp, A. Z. Mustafa, C. Cao, E. J. Wanless, M. H. Stenzel, R. Chapman, *Chem. Sci.* **2025**, *16*, 13807–13815, https://doi.org/10.1039/D5SC04391C.

[55] J. O'Brien, K. J. Shea, *Acc. Chem. Res.* **2016**, *49*, 1200–1210.

[56] M. Nakamoto, T. Nonaka, K. J. Shea, Y. Miura, Y. Hoshino, *J. Am. Chem. Soc.* **2016**, *138*, 4282–4285, https://doi.org/10.1021/jacs.5b12600.
[57] K. Yoshimatsu, B. K. Lesel, Y. Yonamine, J. M. Beierle, Y. Hoshino, K. J. Shea, *Angew. Chem. Int. Ed.* **2012**, *51*, 2405–2408, https://doi.org/10.1002/anie.201107797.
[58] N. Corrigan, K. Jung, G. Moad, C. J. Hawker, K. Matyjaszewski, C. Boyer, *Prog. Polym. Sci.* **2020**, *111*, 101311, https://doi.org/10.1016/j.progpolymsci.2020.101311.
[59] S. Shanmugam, K. Matyjaszewski, Reversible Deactivation Radical Polymerization: State-of-the-Art in 2017. **2018**, pp. 1–39.
[60] J. G. Baker, J. Gloriod, C. A. Figg, *Chem. Sci.* **2025**, *16*, 15298–15309, https://doi.org/10.1039/D5SC04652A.
[61] J.-P. Changeux, A. Christopoulos, *Cell* **2016**, *166*, 1084–1102, https://doi.org/10.1016/j.cell.2016.08.015.
[62] B. P. Cormack, R. H. Valdivia, S. Falkow, *Gene* **1996**, *173*, 33–38.
[63] R. Heim, A. B. Cubitt, R. Y. Tsien, *Nature* **1995**, *373*, 663–664, https://doi.org/10.1038/373663b0.
[64] A. Deng, S. G. Boxer, *J. Am. Chem. Soc.* **2018**, *140*, 375–381, https://doi.org/10.1021/jacs.7b10680.
[65] C.-Y. Lin, M. G. Romei, L. M. Oltrogge, I. I. Mathews, S. G. Boxer, *J. Am. Chem. Soc.* **2019**, *141*, 15250–15265, https://doi.org/10.1021/jacs.9b07152.
[66] A. Kirchhofer, J. Helma, K. Schmidthals, C. Frauer, S. Cui, A. Karcher, M. Pellis, S. Muyldermans, C. S. Casas-Delucchi, M. C. Cardoso, H. Leonhardt, K. P. Hopfner, U. Rothbauer, *Nat. Struct. Mol. Biol.* **2010**, *17*, 133–138, https://doi.org/10.1038/nsmb.1727.
[67] E. Gasteiger, A. Gattiker, C. Hoogland, I. Ivanyi, R. D. Appel, A. Bairoch, *Nucleic. Acids. Res.* **2003**, *31*, 3784–3788, https://doi.org/10.1093/nar/gkg563.
[68] H. Yu, L. Liu, R. Yin, I. Jayapurna, R. Wang, T. Xu, *J. Am. Chem. Soc.* **2024**, *146*, 6178–6188, https://doi.org/10.1021/jacs.3c13909.
[69] M. Asmari, R. Ratih, H. A. Alhazmi, S. El Deeb, *Methods* **2018**, *146*, 107–119, https://doi.org/10.1016/j.ymeth.2018.02.003.
[70] B. Kakasi, E. Gácsi, H. Jankovics, F. Vonderviszt, *BMC Res. Notes* **2023**, *16*, 110, https://doi.org/10.1186/s13104-023-06382-3.
[71] W. F. Harrington, P. Johnson, R. H. Ottewill, *Biochem. J.* **1956**, *62*, 569–582, https://doi.org/10.1042/bj0620569.
[72] A. Laio, M. Parrinello, *Proc. Nat. Acad. Sci. U. S. A* **2002**, *99*, 12562–12566, https://doi.org/10.1073/pnas.202427399.
[73] A. Barducci, G. Bussi, M. Parrinello, *Phys. Rev. Lett.* **2008**, *100*, 020603, https://doi.org/10.1103/PhysRevLett.100.020603.
[74] R. Casasnovas, V. Limongelli, P. Tiwary, P. Carloni, M. Parrinello, *J. Am. Chem. Soc.* **2017**, *139*, 4780–4788, https://doi.org/10.1021/jacs.6b12950.
[75] M. Invernizzi, M. Parrinello, *J. Phys. Chem. Lett.* **2020**, *11*, 2731–2736, https://doi.org/10.1021/acs.jpclett.0c00497.
[76] J. C. Calderón, E. Plut, M. Keller, C. Cabrele, O. Reiser, F. L. Gervasio, T. Clark, *J. Chem. Inf. Model.* **2024**, *64*, 205–218, https://doi.org/10.1021/acs.jcim.3c01574.
[77] V. Leone, F. Marinelli, P. Carloni, M. Parrinello, *Curr. Opin. Struct. Biol.* **2010**, *20*, 148–154, https://doi.org/10.1016/j.sbi.2010.01.011.
[78] Y. Shi, Z. Xia, J. Zhang, R. Best, C. Wu, J. W. Ponder, P. Ren, *J. Chem. Theory Comput.* **2013**, *9*, 4046–4063, https://doi.org/10.1021/ct4003702.
[79] J. J. BelBruno, *Chem. Rev.* **2019**, *119*, 94–119, https://doi.org/10.1021/acs.chemrev.8b00171.
[80] S. Garg, P. Singla, S. Kaur, F. Canfarotta, E. Velliou, J. A. Dawson, N. Kapur, N. J. Warren, S. Amarnath, M. Peeters, *Macromolecules* **2025**, *58*, 1157–1168, https://doi.org/10.1021/acs.macromol.4c01621.
[81] K. Hakobyan, B. B. Noble, J. Xu, *Polym. Chem.* **2023**, *14*, 4116–4125, https://doi.org/10.1039/D3PY00828B.
[82] K. Hakobyan, B. B. Noble, J. Xu, *Prog. Polym. Sci.* **2023**, *147*, 101754, https://doi.org/10.1016/j.progpolymsci.2023.101754.
[83] J. Xu, S. Shanmugam, C. Fu, K.-F. Aguey-Zinsou, C. Boyer, *J. Am. Chem. Soc.* **2016**, *138*, 3094–3106, https://doi.org/10.1021/jacs.5b12408.
[84] J. Xu, C. Fu, S. Shanmugam, C. J. Hawker, G. Moad, C. Boyer, *Angew. Chem. Int. Ed.* **2017**, *56*, 8376–8383, https://doi.org/10.1002/anie.201610223.
[85] J.-F. Lutz, *ACS Macro Lett.* **2014**, *3*, 1020–1023.
[86] A. Al Ouahabi, L. Charles, J.-F. Lutz, *J. Am. Chem. Soc.* **2015**, *137*, 5629–5635, https://doi.org/10.1021/jacs.5b02639.
[87] G. Gody, R. Barbey, M. Danial, S. Perrier, *Polym. Chem.* **2015**, *6*, 1502–1511, https://doi.org/10.1039/C4PY01251H.
[88] G. Gody, T. Maschmeyer, P. B. Zetterlund, S. Perrier, *Nat. Commun.* **2013**, *4*, 2505, https://doi.org/10.1038/ncomms3505.
[89] J. G. Baker, R. Zhang, C. A. Figg, *J. Am. Chem. Soc.* **2024**, *146*, 106–111, https://doi.org/10.1021/jacs.3c12221.
[90] J. G. Baker, S. J. Koehler, K. J. Wood, D. Troya, J. Gloriod, I. C. Anderson, D. C. Gomez, C. A. Figg, *Angew. Chem. Int. Ed.* **2025**, *64*, e202509029, https://doi.org/10.1002/anie.202509029.
[91] T. Junkers, *Macromol. Chem. Phys.* **2017**, *218*, 1600421, https://doi.org/10.1002/macp.201600421.
[92] J. De Neve, J. J. Haven, S. Harrisson, T. Junkers, *Angew. Chem. Int. Ed.* **2019**, *58*, 13869–13873.
[93] C. Zhang, M. W. Bates, Z. Geng, A. E. Levi, D. Vigil, S. M. Barbon, T. Loman, K. T. Delaney, G. H. Fredrickson, C. M. Bates, A. K. Whittaker, C. J. Hawker, *J. Am. Chem. Soc.* **2020**, *142*, 9843–9849.
[94] E. A. Murphy, K. G. Roth, M. W. Bates, M. C. Murphy, J. Edmund, C. M. Bates, C. J. Hawker, *Macromolecules* **2025**, *58*, 8369–8376, https://doi.org/10.1021/acs.macromol.5c01024.
[95] E. A. Murphy, C. Zhang, C. M. Bates, C. J. Hawker, *Acc. Chem. Res.* **2024**, *57*, 1202–1213, https://doi.org/10.1021/acs.accounts.4c00059.
[96] G. P. Smith, V. A. Petrenko, *Chem. Rev.* **1997**, *97*, 391–410, https://doi.org/10.1021/cr960065d.
[97] M. Darmostuk, S. Rimpelova, H. Gbelcova, T. Ruml, *Biotechnol. Adv.* **2015**, *33*, 1141–1161, https://doi.org/10.1016/j.biotechadv.2015.02.008.

Manuscript received: September 11, 2025
Revised manuscript received: October 30, 2025
Manuscript accepted: November 06, 2025
Version of record online: November 17, 2025